J. Fluid Mech. (1992), *vol.* 242, *pp.* 419–440
Printed in Great Britain

A singularity in thermal boundary-layer flow on a horizontal surface

By P. G. DANIELS
Department of Mathematics, City University, Northampton Square, London, EC1V 0HB, UK

(Received 30 September 1991 and in revised form 25 February 1992)

A thermal boundary layer, in which the temperature and velocity fields are coupled by buoyancy, flows along a horizontal, insulated wall. For sufficiently low local Froude number the solution terminates in a singularity with rising skin friction and falling pressure. The structure of the singularity is obtained and the results are compared with numerical solutions of the horizontal boundary-layer equations. A novel feature of the analysis is that the powers of the streamwise coordinate involved in the structure of the singularity do not appear to be simple rational numbers and are determined from the solution of a pair of ordinary differential equations which govern the flow in an inner viscous region close to the wall. Modifications of the theory are noted for cases where either the temperature or a non-zero heat transfer are specified at the wall.

1. Introduction

In classical boundary-layer theory an adverse pressure gradient associated with decelerating external flow heralds the occurrence of the Goldstein (1948) singularity. In general this leads to the breakdown of a global high-Reynolds-number theory based on a minor viscous adjustment to the Euler solution in a region confined to the neighbourhood of a solid body. Although the resolution of the difficulty lies in a completely new structure (Stewartson 1970; Smith 1982) in which the Goldstein singularity is avoided, the existence of the singularity and more generally a full understanding of the properties of the boundary-layer equations have played a central role in the determination of high-Reynolds-number flows. In buoyancy-free boundary layers the pressure gradient is known from the external flow and the removal of this constraint on a short streamwise lengthscale (Stewartson & Williams 1969; Messiter 1970) allows separation to occur smoothly, thereby avoiding the Goldstein singularity. However, in horizontal thermal boundary layers where buoyancy has a significant effect on the flow field the pressure gradient generally varies with depth in the layer so that although it is predetermined at the edge of the boundary layer it must otherwise be found as part of the solution process, along with both the temperature and velocity fields. A Goldstein singularity is no longer necessarily appropriate and the present paper addresses the question of what type of singularity may occur in a buoyant thermal boundary layer on a horizontal wall.

There is a considerable body of work concerned with the nature of singularities of the boundary-layer equations at separation in natural convective flows on vertical plates. Merkin (1969) performed numerical calculations for an isothermal plate while Wilks (1974) and Hunt & Wilks (1980) considered both constant-heat-flux and constant-temperature boundary conditions. Further work by Messiter & Linan (1976), Merkin (1983) and Ingham (1985) has considered the effects of leading and

trailing edges, perturbations to the temperature and geometry of the plate surface and sudden heating. Previous theoretical studies of buoyancy effects in horizontal thermal boundary layers have concentrated on flows generated by a uniformly heated or cooled plate. Stewartson (1958) considered an isothermal semi-infinite plate and his results as interpreted by Gill, Zeh & del Casal (1965) established the existence of similarity solutions only for the boundary layer above a heated surface or below a cooled surface. Theoretical work on the cooled upward-facing (or heated downward-facing) plate has been carried out using an integral analysis by Clifton & Chapman (1969). Jones (1973) and Pera & Gebhart (1973) considered the effect of a small inclination of the plate, while effects of mass transfer from the plate have been incorporated by Bandrowski & Rybski (1976) (see also Kerr 1980) and non-Boussinesq effects by Ackroyd (1976). Experimental work on free convection from heated or cooled plates has been reported by Rotem & Claassen (1969), Aihara, Yamada & Endo (1972), Goldstein, Sparrow & Jones (1973), Restrepo & Glicksman (1974), Al-Arabi & El-Riedy (1976), Faw & Dullforce (1981) and Hatfield & Edwards (1981). Further experimental work and numerical calculations have also been carried out by Goldstein & Lau (1983).

There seems to have been little previous theoretical work on buoyancy effects for thermal boundary layers on insulated horizontal walls. Such layers may exist, for example, within a thermal cavity flow driven by lateral heating (Bejan, Al-Homoud & Imberger 1981; Simpkins & Chen 1986; Patterson & Armfield 1990) where fluid emerges from the vicinity of the lower cold and upper hot corners of the cavity in the form of 'intrusion' jets. In the boundary layers established on the horizontal insulated walls the flow takes place within a stable stratification as the isotherms descending near the cold wall and ascending near the hot wall are convected around the corners and along the horizontal boundaries. The thermal environment is comparable to that of the flow above a cooled horizontal plate or below a heated plate, the statically stable situation in which, as mentioned above, a similarity solution does not exist for natural convective flow (Gill *et al.* 1965). However such a boundary layer can exist if inertial effects are sufficiently strong, such as those resulting from a jet-like flow upstream or from an external velocity at the edge of the boundary layer. These requirements are essentially equivalent to a sufficiently high Froude number for the flow, the Froude number being a measure of the importance of inertia, as supplied by the external flow, relative to the adverse pressure gradient due to buoyancy. In situations where the flow is initiated by strong inertial effects the Froude number is effectively dependent on the downstream location in the boundary layer, leading to the possibility of a termination of the boundary-layer solution if, as the flow proceeds, its value falls below a critical level.

Evidence that under certain circumstances a buoyant horizontal boundary layer terminates in a singularity has been found in finite-difference computations of the relevant partial differential equations by Gargaro (1991), who considered a boundary layer on an insulated horizontal wall driven by a constant external velocity. Consideration of possible downstream asymptotes confirms that similarity solutions do not exist for sufficiently low Froude number (Daniels, Blythe & Simpkins 1987) and Gargaro's calculations show that in many circumstances the boundary layer, initiated by appropriate velocity and temperature profiles at $x = 0$, terminates in a singularity at a finite value of the streamwise coordinate, $x = x_0$. Furthermore the singularity is not associated with a point of separation but with a sudden rise in skin friction.

In §2 the governing equations and boundary conditions for the horizontal

boundary-layer flow are formulated. The similarity solution described by Daniels *et al.* (1987) is briefly discussed and is shown to indicate the possibility of a singularity of the boundary-layer equations when interpreted in the sense of a slowly varying approximation. The actual structure of the singularity is proposed in §3 and requires consideration of inner and outer regions of the boundary layer in the limit as $x \to x_0-$. The streamwise variation in the outer region is primarily inviscid and the inner viscous region is needed to ensure that the boundary conditions at the wall are satisfied.

In the outer region the equations reduce to a second-order Sturm–Liouville eigenvalue problem, which is discussed in §4. It is the existence of a solution to this problem at a given downstream location in the boundary layer that determines whether and where the singularity occurs. This position is related to the value of a local Froude number for the flow. The overall structure and streamwise variation of the solution as the singularity is approached are only determined when the solutions for the flow and temperature fields in the inner viscous region have been found. Buoyancy does not affect the inner flow to leading order and so the velocity and temperature fields can be considered separately: the inner flow field is determined in §5 and the inner temperature field in §6. Minor modifications needed to allow for a non-zero heat flux at the wall or a specified wall temperature are also noted. A discussion of the results in §7 includes a comparison with Gargaro's (1991) numerical computations.

2. Formulation

Consider two-dimensional motion in a fluid of mean density ρ, kinematic viscosity ν, thermal diffusivity κ and coefficient of thermal expansion α^* set up by velocity and temperature profiles of vertical scale $z^* \sim h$ along an insulated horizontal wall which coincides with the x^*-axis. Away from the wall the flow has constant speed U_0^* in the x^*-direction and constant temperature T_0^*. In the Boussinesq approximation the governing equations for steady flow are

$$\frac{\partial \bar{u}}{\partial \bar{x}} + \frac{\partial \bar{w}}{\partial \bar{z}} = 0, \tag{2.1}$$

$$\bar{u}\frac{\partial \bar{u}}{\partial \bar{x}} + \bar{w}\frac{\partial \bar{u}}{\partial \bar{z}} = -\frac{\partial \bar{p}}{\partial \bar{x}} + \nabla^2 \bar{u}, \tag{2.2}$$

$$\bar{u}\frac{\partial \bar{w}}{\partial \bar{x}} + \bar{w}\frac{\partial \bar{w}}{\partial \bar{z}} = -\frac{\partial \bar{p}}{\partial \bar{z}} + \nabla^2 \bar{w} + R\sigma^{-1}\bar{T}, \tag{2.3}$$

$$\bar{u}\frac{\partial \bar{T}}{\partial \bar{x}} + \bar{w}\frac{\partial \bar{T}}{\partial \bar{z}} = \sigma^{-1}\nabla^2 \bar{T}, \tag{2.4}$$

where the velocity components $\bar{u}$, $\bar{w}$ are made non-dimensional by ν/h, $(x^*, z^*) = h(\bar{x}, \bar{z})$ and the pressure and temperature fields are given by

$$p^* = -\rho g^* z^* + (\rho \nu^2/h^2)\,\bar{p}(\bar{x}, \bar{z}), \tag{2.5}$$

$$T^* = T_0^* + T_0^*\,\bar{T}(\bar{x}, \bar{z}), \tag{2.6}$$

where g^* is the acceleration due to gravity which acts in the negative z^*-direction. The two parameters appearing in (2.3) and (2.4) are the Rayleigh number and Prandtl number defined by

$$R = \alpha^* g^* T_0^* h^3/\nu\kappa, \quad \sigma = \nu/\kappa, \tag{2.7}$$

respectively.

In the limit of large Rayleigh number and large external flow the motion assumes a boundary-layer form in which

$$\left.\begin{aligned} \bar{T} = T(x,z)+\ldots, \quad \bar{p} = Rp(x,z)+\ldots, \quad \bar{u} = R^{\frac{1}{2}}u(x,z)+\ldots, \\ \bar{w} = w(x,z)+\ldots \quad (R \gg 1), \end{aligned}\right\} \tag{2.8}$$

where $\bar{x} = R^{\frac{1}{2}}x$ and $\bar{z} = z$. Assuming that

$$U_0^* = R^{\frac{1}{2}}U\nu/h \quad (R \gg 1) \tag{2.9}$$

the boundary-layer problem is to solve

$$\frac{\partial u}{\partial x}+\frac{\partial w}{\partial z} = 0, \tag{2.10}$$

$$u\frac{\partial u}{\partial x}+w\frac{\partial u}{\partial z} = -\frac{\partial p}{\partial x}+\frac{\partial^2 u}{\partial z^2}, \tag{2.11}$$

$$0 = -\frac{\partial p}{\partial z}+\sigma^{-1}T, \tag{2.12}$$

$$u\frac{\partial T}{\partial x}+w\frac{\partial T}{\partial z} = \sigma^{-1}\frac{\partial^2 T}{\partial z^2}, \tag{2.13}$$

subject to

$$u = w = \frac{\partial T}{\partial z} = 0 \quad \text{on} \quad z = 0, \tag{2.14}$$

$$T \to 0, \quad p \to 0, \quad u \to U \quad \text{as} \quad z \to \infty \tag{2.15}$$

and

$$u = \tilde{U}(z), \quad T = \tilde{T}(z) \quad \text{at} \quad x = 0. \tag{2.16}$$

Here $\tilde{U}$ and $\tilde{T}$ are velocity and temperature profiles with $\tilde{U} > 0$ and $\tilde{T} < 0$ so that the boundary layer is initiated by forward flow with a statically stable stratification.

A stream function ψ is introduced such that

$$u = \frac{\partial \psi}{\partial z}, \quad w = -\frac{\partial \psi}{\partial x} \tag{2.17}$$

and it can be established from (2.13), (2.14) and (2.15) that the heat-flux integral

$$\int_0^\infty \psi\frac{\partial T}{\partial z}\mathrm{d}z = Q \tag{2.18}$$

is constant for all values of x in the boundary layer. This represents the fact that no heat can escape from the edge of the boundary layer or through the insulated wall.

Solutions of the thermal boundary-layer problem (2.10)–(2.16) have been computed by Gargaro (1991) although the initial profiles (2.16) were replaced by forms equivalent to the occurrence of a non-buoyant jet flow upstream, of the type first analysed by Glauert (1956), equivalent to the behaviour

$$\psi \sim x^{\frac{1}{4}}\phi(\mu), \quad T \sim x^{-\frac{1}{4}}\theta(\mu) \quad (\phi \geqslant 0, \theta < 0) \tag{2.19}$$

as $x \to 0$, where $\mu = z/x^{\frac{3}{4}}$ and ϕ and θ are known functions of μ. In any event the constant Q can be determined by evaluation of the integral (2.18) as $x \to 0$. Gargaro's calculations based on finite differences and a downstream marching procedure show that if U is sufficiently large the flow develops smoothly downstream and ultimately attains a similarity form in which

$$\psi \sim x^{\frac{1}{2}}F(\zeta), \quad T \sim x^{-\frac{1}{2}}G(\zeta) \tag{2.20}$$

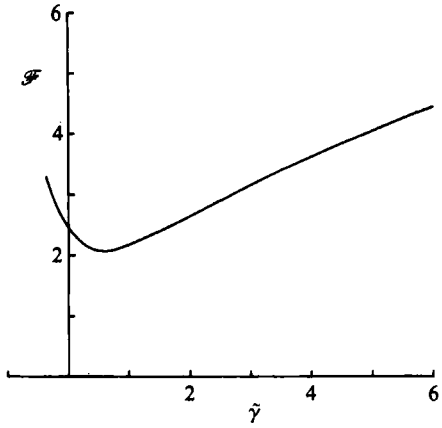

FIGURE 1. Solution of (2.25)–(2.28) showing $\mathscr{F}$ as a function of $\tilde{\gamma}$ for $\sigma = 1$.

as $x \to \infty$, where $\zeta = z/x^{\frac{1}{3}}$. Here from (2.13)–(2.15)

$$G = -\Omega \exp\left(-\tfrac{1}{2}\sigma \int_0^\zeta F \,\mathrm{d}\zeta\right), \tag{2.21}$$

where Ω is a constant and F satisfies

$$F''' + \tfrac{1}{2}FF'' = \tfrac{1}{2}\zeta\sigma^{-1}\Omega \exp\left(-\tfrac{1}{2}\sigma \int_0^\zeta F \,\mathrm{d}\zeta\right), \tag{2.22}$$

with
$$F = F' = 0 \quad (\zeta = 0), \quad F' \to U \quad (\zeta \to \infty). \tag{2.23}$$

From (2.18),

$$\tfrac{1}{2}\Omega\sigma \int_0^\infty F^2 \exp\left(-\tfrac{1}{2}\sigma \int_0^\zeta F \,\mathrm{d}\zeta\right)\mathrm{d}\zeta = Q. \tag{2.24}$$

By making transformations $\Omega = Q^{\frac{1}{3}}\tilde{\Omega}$, $F = \Omega^{\frac{1}{3}}\tilde{F}(\tilde{\zeta})$, $\zeta = \Omega^{-\frac{1}{3}}\tilde{\zeta}$, equation (2.22) becomes

$$\tilde{F}''' + \tfrac{1}{2}\tilde{F}\tilde{F}'' = \tfrac{1}{2}\tilde{\zeta}\sigma^{-1} \exp\left(-\tfrac{1}{2}\sigma \int_0^{\tilde{\zeta}} \tilde{F} \,\mathrm{d}\tilde{\zeta}\right) \tag{2.25}$$

and can be solved subject to

$$\tilde{F} = \tilde{F}' = 0, \quad \tilde{F}'' = \tilde{\gamma} \quad (\tilde{\zeta} = 0) \tag{2.26}$$

for a range of values of $\tilde{\gamma}$ to obtain

$$\mathscr{F} = U/Q^{\frac{1}{3}} = \tilde{\Omega}^{\frac{2}{3}}\tilde{F}'(\infty), \tag{2.27}$$

where from (2.24) $\tilde{\Omega}$ is determined by

$$\tilde{\Omega}^{\frac{4}{3}} = 2\Big/\left\{\sigma \int_0^\infty \tilde{F}^2 \exp\left(-\tfrac{1}{2}\sigma \int_0^{\tilde{\zeta}} \tilde{F} \,\mathrm{d}\tilde{\zeta}\right)\mathrm{d}\tilde{\zeta}\right\}. \tag{2.28}$$

Computations described by Daniels *et al.* (1987) indicate the existence of dual solutions for $\mathscr{F}$ above a critical value $\mathscr{F}_0(\sigma)$. Results for unit Prandtl number are shown in figure 1, and $\mathscr{F}_0(1) \approx 2.1$; the parameter $\mathscr{F}$ is associated with the Froude number of the flow. Non-existence of a solution in the absence of external flow ($\mathscr{F} = 0$) can be compared to the equivalent result for an isothermal plate obtained by Stewartson (1958) and Gill *et al.* (1965).

The above results indicate that the boundary-layer flow may be sustainable as x increases indefinitely when $U/Q^{\frac{1}{3}}$ is greater than $\mathscr{F}_0(\sigma)$. In Gargaro's computations,

as the flow evolves from the initial jet profile (2.19) the wall temperature rises and the velocity decreases in the adverse pressure gradient

$$\frac{\partial p}{\partial x} = -\frac{1}{\sigma}\int_z^\infty \frac{\partial T}{\partial x}\mathrm{d}z \sim -\frac{x^{-\frac{5}{4}}}{\sigma}\left\{\tfrac{3}{4}\mu\theta + \tfrac{1}{2}\int_\mu^\infty \theta\,\mathrm{d}\mu\right\} > 0 \quad (x\to 0), \tag{2.29}$$

generated by buoyancy. At very low values of $U/Q^{\frac{1}{3}}$ this results in the onset of reverse flow within the boundary layer, at which point the computation is unable to proceed further downstream. However, at higher values of $U/Q^{\frac{1}{3}}$ a forward flow is maintained which ultimately terminates in a singularity at a finite value of x. The singularity is characterized by a sudden rise in the skin friction associated with a rapid drop in the pressure and a decrease in the displacement thickness of the boundary layer. At sufficiently high values of $U/Q^{\frac{1}{3}}$ the singularity is avoided and the flow is able to attain the asymptotic form (2.20) as $x\to\infty$.

The similarity solution (2.20) can be used as the basis for an approximate method of predicting the existence of a singularity in the boundary layer by considering $\mathscr{F}$ to be a slowly-decreasing function of x. This will be equivalent, for example, to a slowly decelerating external stream and the skin friction $\gamma = F''(0)$ will fall, following the right-hand branch of figure 1, until it reaches the value γ_0 at which $\mathscr{F} = \mathscr{F}_0$. There,

$$\left.\begin{aligned} F &= F_0(\zeta) + (\gamma-\gamma_0)F_1(\zeta) + \ldots, \\ \Omega &= \Omega_0 + (\gamma-\gamma_0)\Omega_1 + \ldots, \\ \mathscr{F} &= \mathscr{F}_0 + (\gamma-\gamma_0)^2\mathscr{F}_1 + \ldots, \end{aligned}\right\} \tag{2.30}$$

where $F_1 = \partial F/\partial\gamma(\gamma=\gamma_0)$ and $\Omega_1 = \mathrm{d}\Omega/\mathrm{d}\gamma(\gamma=\gamma_0)$. The situation can be compared to that in a classical boundary-layer flow driven by an external velocity $x^{\mathscr{F}}$, where F is the solution of the Falkner–Skan equation and solutions exist for $\mathscr{F} > \mathscr{F}_0 = -0.0904$ (Hartree 1937; Stewartson 1954). Then $F_1 = \partial F/\partial\gamma(\gamma=\gamma_0) = -\mathscr{F}_0^{-1}F_0'$ and since the requirement that $F_1'(0) = 0$ is equivalent to $F_0''(0) = 0$ it follows that $\gamma_0 = 0$, and the singularity corresponds to the point of separation of the boundary layer. In the thermal boundary layer, however, it is readily established that F_1 is not proportional to F_0' owing to the presence of the term which explicitly involves ζ on the right-hand side of (2.22). As a result, $\gamma_0 > 0$ and the singular behaviour of F as a function of $\mathscr{F}$ represented by (2.30) does not correspond to a point of separation. This is also a property of the exact structure of the singularity to be considered next.

3. Structure of the singularity at x_0

Consider now the solution of the thermal boundary-layer equations (2.10)–(2.16) subject to a constant external velocity U, heat flux Q and Prandtl number σ such that as the solution proceeds downstream from the initial profile (2.16) or (2.19) a singularity develops at $x = x_0$. In the main part of the boundary layer it is assumed that the flow has the form

$$\left.\begin{aligned} \psi &= \psi_0(z) + X^a\psi_1(z) + \ldots, \quad u = u_0(z) + X^a u_1(z) + \ldots, \\ p &= p_0(z) + X^a p_1(z) + \ldots, \quad T = T_0(z) + X^a T_1(z) + \ldots, \end{aligned}\right\} \tag{3.1}$$

as $X\to 0$, where $X = x_0 - x$ and a is a constant to be determined. Here

$$u_0 = \psi_0', \quad p_0 = -\frac{1}{\sigma}\int_z^\infty T_0\,\mathrm{d}z, \tag{3.2}$$

with $u_0(\infty) = U$, and it is supposed that

$$\psi_0 \sim \alpha z^b, \quad T_0 \sim T_0(0) + \beta z^c \quad \text{as} \quad z \to 0, \tag{3.3}$$

where b and c are further constants to be determined and $\alpha, \beta > 0$. Provided that $a < 1$ all of the functions appearing in (3.1) are solutions of the inviscid equations, suggesting that an inner region will occur in which viscosity balances inertia and in which the flow is driven at least partly by the streamwise pressure gradient $\partial p/\partial x$.

If this inner region is of thickness $z \sim X^d$ as $X \to 0$ it is necessary that $b > 1$,

$$d = 1/(b+1), \quad a = 2(b-1)/(b+1) \tag{3.4}$$

and then in the inner region

$$\left.\begin{aligned} \psi &= X^{b/(1+b)} f(\eta) + \ldots, \\ T &= T_0(0) + X^{c/(1+b)} g(\eta) + \ldots, \\ p &= p_0(0) + X^{2(b-1)/(b+1)} q(\eta) + \ldots, \end{aligned}\right\} \tag{3.5}$$

as $X \to 0$ where $\eta = z/X^{1/(1+b)}$. Substitution into (2.11), (2.12) then shows that if $b < \frac{3}{2}$

$$q(\eta) = q \quad \text{(constant)} \tag{3.6}$$

and that

$$f''' - \frac{b}{b+1} f f'' + \frac{b-1}{b+1} f'^2 = -\frac{2(b-1)}{b+1} q. \tag{3.7}$$

Boundary conditions for f require no slip at the wall,

$$f = f' = 0 \quad (\eta = 0), \tag{3.8}$$

and matching with the outer solution for ψ_0:

$$f \sim \alpha \eta^b \quad (\eta \to \infty). \tag{3.9}$$

Similarly from (2.13) the inner temperature function g satisfies

$$g'' - \frac{\sigma}{1+b}(bfg' - cf'g) = 0 \tag{3.10}$$

with boundary conditions

$$g' = 0 \quad (\eta = 0), \qquad g \sim \beta \eta^c \quad (\eta \to \infty). \tag{3.11}$$

For $b > 1$ the general form of the solution for f as $\eta \to \infty$ is

$$f \sim k_1 \eta^b + k_2 \eta^{2-b} + k_3 \eta^{b-1} + k_4 \eta^{4-3b}, \tag{3.12}$$

where k_1 and k_3 are arbitrary constants and

$$k_2 = \frac{q}{k_1 b(2b-3)}, \quad k_4 = \frac{k_2^2(2-b)}{2bk_1(4b-5)}. \tag{3.13}$$

The constant k_3 corresponds to an origin shift in η and the ordering of terms in (3.12) assumes $\frac{5}{4} < b < \frac{3}{2}$, to be confirmed below. From (3.9) it is required that $k_1 = \alpha > 0$ and for a given value of b it is possible to select q to avoid f approaching infinity at finite η or a negative form proportional to η^b as $\eta \to \infty$. As a result of this both q and

$$k_3 = k_3(b) \tag{3.14}$$

are determined from the numerical solution for f.

In the outer region substitution of (3.1) into (2.11)–(2.13) gives

$$u_0'\psi_1 - u_0 u_1 = p_1, \quad p_1' = T_1/\sigma, \quad u_0 T_1 - T_0'\psi_1 = 0, \tag{3.15}$$

so that

$$T_1 = T_0'\psi_1/u_0, \quad p_1 = -\frac{1}{\sigma}\int_z^\infty T_1\,\mathrm{d}z \tag{3.16}$$

and ψ_1 satisfies

$$u_0\psi_1' - u_0'\psi_1 = \frac{1}{\sigma}\int_z^\infty \frac{T_0'\psi_1}{u_0}\mathrm{d}z. \tag{3.17}$$

This equation for ψ_1 must be solved subject to

$$\psi_1/z^{b-1} \to 0 \quad \text{as} \quad z \to 0, \tag{3.18}$$

in order that when $b < \frac{3}{2}$ an inner solution for ψ is not generated larger than that already assumed in (3.5). Provided there exists a solution of (3.17) and (3.18) it follows that

$$\psi_1 \sim d_1 z^{2-b} \quad \text{as} \quad z \to 0, \tag{3.19}$$

where d_1 is a constant which must be chosen as

$$d_1 = \frac{q}{\alpha b(2b-3)}, \tag{3.20}$$

in order that the solution matches consistently with the term $k_2\eta^{2-b}$ in the inner solution for f. From (3.16) and (3.17) this also ensures that near the wall the outer pressure $p_1(0) = q$ drives the inner flow. The eigenvalue problem (3.17), (3.18) is discussed in §4.

It remains to find the two constants b and c which determine the form of the boundary-layer profiles ψ_0 and T_0 near the wall and, through the relations (3.4), the extent of the inner region and the streamwise gradients in the outer solution. The value of b is fixed by the requirement that in the solution for f

$$k_3(b) = 0, \tag{3.21}$$

and in §5 it will be shown that such a value exists in the range $\frac{5}{4} < b < \frac{3}{2}$. If k_3 were non-zero the inner form (3.12) would generate corrections in the outer solutions (3.1) of order $X^{1/(1+b)}$. The corresponding function of z in the solution for the stream function would satisfy the same equation as that for ψ_1 but would need to have the form $k_3 z^{b-1}$ as $z \to 0$. Such a solution would not exist because the profiles u_0 and T_0 are precisely those for which the solution has the behaviour (3.18) as $z \to 0$.

Finally the value of c is fixed by the requirement that in the solution for g an exponentially large form is avoided as $\eta \to \infty$. Computations of c for a range of Prandtl numbers are described in §6.

4. Outer eigenvalue problem

The occurrence of the singularity is fundamentally linked to the existence of an eigensolution of the system (3.17), (3.18) when $b < \frac{3}{2}$, an alternative form of which can be obtained by differentiation, giving

$$u_0\psi_1'' - u_0''\psi_1 = -\frac{T_0'}{\sigma u_0}\psi_1, \tag{4.1}$$

with

$$\psi_1/z^{b-1} \to 0 \quad (z \to 0), \qquad \psi_1' \to 0 \quad (z \to \infty). \tag{4.2}$$

This may be further simplified by setting

$$\psi_1 = u_0 \Psi(z), \tag{4.3}$$

so that Ψ satisfies the second-order Sturm–Liouville self-adjoint eigenvalue problem (see for example Ross 1964, p. 414)

$$\frac{\mathrm{d}}{\mathrm{d}z}(u_0^2 \Psi') + \sigma^{-1} T_0' \Psi = 0, \tag{4.4}$$

with boundary conditions

$$\Psi \to 0 \quad (z \to 0), \qquad \Psi' \to 0 \quad (z \to \infty). \tag{4.5}$$

At infinity Ψ must approach a constant value while at the origin non-zero solutions must be excluded. The eigenvalue can be regarded as the downstream location x_0 at which the boundary-layer profiles u_0 and T_0' are such as to allow the existence of an eigensolution, but of course in a typical boundary-layer calculation these profiles are not known analytically. Although an explicit solution of the system does not appear to be possible, progress can be made by two approximate methods, one based on an assumption that σ is large and another on the assumption of simplified analytical forms for u_0 and T_0'.

First assume that u_0 and T_0 are arbitrary finite functions of z and that σ is large. Then Ψ can be approximated by an expansion

$$\Psi = \Psi_0(z) + \sigma^{-1} \Psi_1(z) + \ldots, \tag{4.6}$$

and substitution into (4.4) and use of the boundary condition at infinity gives at leading order

$$\Psi_0(z) = C_0, \tag{4.7}$$

where C_0 is a constant. At order σ^{-1}, $\Psi_1(\infty)$ may be taken as zero assuming that $\Psi(\infty) = C_0$ is used as a normalization for Ψ, and then

$$\Psi_1(z) = C_0 \int_z^\infty T_0 u_0^{-2} \, \mathrm{d}z. \tag{4.8}$$

Now as $z \to 0$,

$$\Psi \sim C_0 \left\{ 1 + \sigma^{-1} \left(\int_0^\infty T_0 u_0^{-2} \, \mathrm{d}z - \frac{T_0(0)}{\alpha^2 b^2 (3-2b)} z^{3-2b} + \ldots \right) + \ldots \right\}. \tag{4.9}$$

Since $T_0 < 0$ and $u_0^2 > 0$ this result shows that the combined effect of buoyancy and forward flow is to reduce the value of $\Psi(0)$, suggesting the possibility of its value reaching zero for sufficiently low forward velocity (u_0), sufficiently low Prandtl number or sufficiently high buoyancy (T_0). The result (4.9) is no longer formally valid when σ is finite but as an approximate estimate it suggests that an eigenfunction and hence the singularity will exist when the flow reaches a point at which

$$\frac{1}{\sigma} \int_0^\infty \frac{|T_0|}{u_0^2} \mathrm{d}z = 1. \tag{4.10}$$

The combination on the left-hand side is effectively a local Richardson number or the square of a local inverse Froude number for the flow (Turner 1973, p.12) and when its value has risen sufficiently high the singularity will develop within the boundary layer. Note that in (4.9) the term in z^{3-2b} provides the correct behaviour for ψ_1 as $z \to 0$, as given by (3.19) and (3.20), provided

$$C_0 = \sigma q / T_0(0). \tag{4.11}$$

A second method of analysing the eigenvalue problem (4.4), (4.5) is to replace u_0 and T_0' by elementary functions. Simple forms with the correct type of behaviour as $z \to \infty$ are

$$u_0 = \hat{U}, \quad T_0' = (\hat{T}/l)\exp(-z/l), \tag{4.12}$$

where $\hat{U}$, $\hat{T}$ and l are constants. These forms correspond to behaviour at the origin equivalent to $b = 1$ and $c = 1$ in (3.3) which are not the correct values to be identified in §5 below. However, the general solution of the resulting eigenvalue equation

$$\Psi'' + \left(\frac{\hat{T}}{\sigma l \hat{U}^2}\right) e^{-z/l}\,\Psi = 0 \tag{4.13}$$

is

$$\Psi = A_0 J_0(\chi) + B_0 Y_0(\chi), \tag{4.14}$$

where

$$\chi = \frac{2\hat{T}^{\frac{1}{2}} l^{\frac{1}{2}}}{\sigma^{\frac{1}{2}} \hat{U}} e^{-z/2l} \tag{4.15}$$

and application of the boundary conditions (4.5) gives $B_0 = 0$ and

$$\frac{2\hat{T}^{\frac{1}{2}} l^{\frac{1}{2}}}{\sigma^{\frac{1}{2}} \hat{U}} = \chi_n, \quad n = 1, 2\ldots, \tag{4.16}$$

where χ_n is the nth zero of the Bessel function J_0. Thus an infinite set of eigenfunctions is identified as the effective local inverse Froude number $(\hat{T}l/\sigma\hat{U}^2)^{\frac{1}{2}}$ increases. In a boundary-layer computation starting from high Froude number, as in Gargaro's (1991) calculations, the singularity will develop at the point corresponding to the lowest zero, $\chi_1 = 2.4048$.

5. Inner flow field

Here it is established that for a certain value of b in the range $\frac{5}{4} < b < \frac{3}{2}$ there is a solution of the inner problem (3.7)–(3.9) for f for which $k_3 = 0$. It is convenient to introduce a transformation

$$f(\eta) = (\bar{\alpha}/\alpha)^{-1/(b+1)} \bar{f}(\bar{\eta}), \quad q = (\bar{\alpha}/\alpha)^{-4/(b+1)} \bar{q}, \quad \eta = (\bar{\alpha}/\alpha)^{1/(b+1)} \bar{\eta}, \tag{5.1}$$

so that $\bar{f}$ satisfies

$$\bar{f}''' - \frac{b}{b+1}\bar{f}\bar{f}'' + \frac{b-1}{b+1}\bar{f}'^2 = -\frac{2(b-1)}{b+1}\bar{q} \tag{5.2}$$

and at the origin is assumed to have the behaviour

$$\bar{f} = \bar{f}' = 0, \quad \bar{f}'' = 1 \quad (\bar{\eta} = 0). \tag{5.3}$$

Solutions can then be computed numerically from $\bar{\eta} = 0$ and for a given value of b, $\bar{q}$ can be chosen to avoid an infinite singularity in $\bar{f}$ at finite $\bar{\eta}$ or a negative form proportional to $\bar{\eta}^b$ as $\bar{\eta} \to \infty$, as shown in figure 2. For this value of $\bar{q}$, $\bar{f}$ has the form

$$\bar{f} \sim \bar{k}_1 \bar{\eta}^b + \bar{k}_2 \bar{\eta}^{2-b} + \bar{k}_3 \bar{\eta}^{b-1} + \bar{k}_4 \bar{\eta}^{4-3b} \quad (\bar{k}_1 > 0), \tag{5.4}$$

as $\bar{\eta} \to \infty$ and by defining $\bar{\alpha} = \bar{k}_1$ in (5.1) the solution for f has the behaviour $f \sim \alpha\eta^b$ as $\eta \to \infty$, as required by (3.9). In (5.4) the constants $\bar{k}_2$ and $\bar{k}_4$ are given by

$$\bar{k}_2 = \frac{\bar{q}}{\bar{k}_1 b(2b-3)}, \quad \bar{k}_4 = \frac{\bar{k}_2^2(2-b)}{2b\bar{k}_1(4b-5)}, \tag{5.5}$$

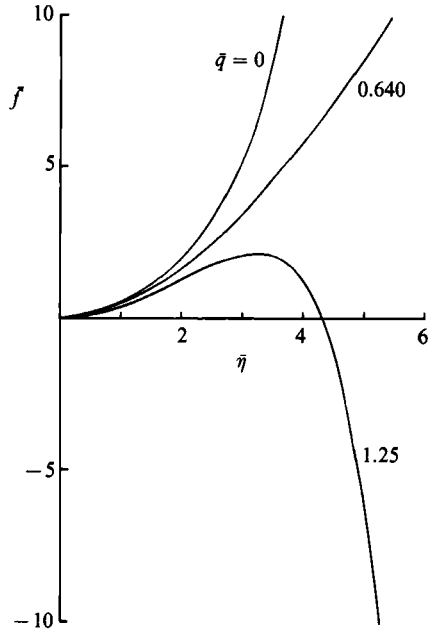

FIGURE 2. Solution of (5.2), (5.3) for $b = \frac{3}{2}$ showing how $\bar{q}$ is chosen to ensure $\bar{f} \sim \bar{k}_1 \bar{\eta}^b$ as $\bar{\eta} \to \infty$.

but like $\bar{k}_1$, the value of $\bar{k}_3$ can only be determined from the overall solution for $\bar{f}$.

For general b in the range $\frac{5}{4} < b < \frac{3}{2}$ the value of $\bar{k}_3$ is non-zero and it is possible to obtain analytical predictions of its form in the two limiting cases $b \to \frac{3}{2}$ and $b \to \frac{5}{4}$. In order to investigate the former limit it is convenient to set $b = \frac{3}{2} - \delta$ and then from (5.4)

$$\bar{f} \sim \bar{k}_1 \bar{\eta}^{\frac{3}{2}}(1 - \delta \ln \bar{\eta} + \ldots) + \bar{k}_2 \bar{\eta}^{\frac{1}{2}}(1 + \delta \ln \bar{\eta} + \ldots) + \bar{k}_3 \bar{\eta}^{\frac{1}{2}}(1 - \delta \ln \bar{\eta} + \ldots) \quad (\bar{\eta} \to \infty). \tag{5.6}$$

When $b = \frac{3}{2}$ equation (5.2) becomes

$$\bar{f}''' - \tfrac{3}{5}\bar{f}\bar{f}'' + \tfrac{1}{5}\bar{f}'^2 = -\tfrac{2}{5}\bar{q} \tag{5.7}$$

and the positive solution which satisfies (5.3) and approaches $\bar{k}_1 \bar{\eta}^{\frac{3}{2}}$ as $\bar{\eta} \to \infty$ has the form

$$\bar{f} \sim \bar{k}_1 \bar{\eta}^{\frac{3}{2}} + k_0 \bar{\eta}^{\frac{1}{2}} \ln \bar{\eta} + k \bar{\eta}^{\frac{1}{2}} \quad (\bar{\eta} \to \infty), \tag{5.8}$$

where $k_0 = -2\bar{q}/3\bar{k}_1$, $\bar{k}_1 > 0$ and from a numerical solution of (5.7), $\bar{q} \approx 0.640$. Comparison of (5.6) and (5.8) gives to leading order $\bar{k}_2 + \bar{k}_3 = k$ and $\delta(\bar{k}_2 - \bar{k}_3) = k_0$ which implies that in particular

$$\bar{k}_3 \sim -\tfrac{1}{2}k_0(\tfrac{3}{2} - b)^{-1} \quad (b \to \tfrac{3}{2}) \tag{5.9}$$

and since $k_0 < 0$, this shows that $\bar{k}_3$ becomes large and positive as $b \to \frac{3}{2}-$.

In order to investigate the limit $b \to \frac{5}{4}$ it is convenient to set $b = \frac{5}{4} + \delta$ and then from (5.4)

$$\bar{f} \sim \bar{k}_1 \bar{\eta}^{\frac{5}{4}}(1 + \delta \ln \bar{\eta} + \ldots) + \bar{k}_2 \bar{\eta}^{\frac{3}{4}}(1 - \delta \ln \bar{\eta} + \ldots) + \bar{k}_3 \bar{\eta}^{\frac{1}{4}}(1 + \delta \ln \bar{\eta} + \ldots) + \bar{k}_4 \bar{\eta}^{\frac{1}{4}}(1 - 3\delta \ln \bar{\eta} + \ldots) \quad (\bar{\eta} \to \infty). \tag{5.10}$$

When $b = \frac{5}{4}$ equation (5.2) becomes

$$\bar{f}''' - \tfrac{5}{9}\bar{f}\bar{f}'' + \tfrac{1}{9}\bar{f}'^2 = -\tfrac{2}{9}\bar{q} \tag{5.11}$$

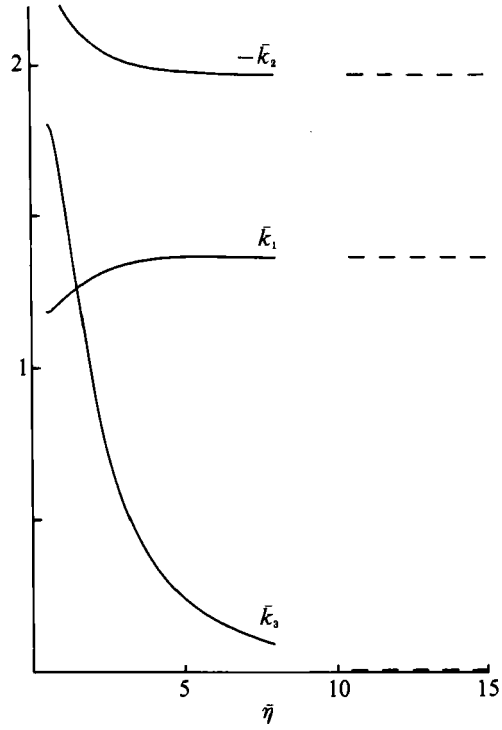

FIGURE 3. Convergence of $\bar{k}_1, \bar{k}_2, \bar{k}_3$ for $b = 1.36$, $\bar{q} = 1.024$ by equating the numerical solutions for $\bar{f}$, $\bar{\eta}\bar{f}'$, $\bar{\eta}^2\bar{f}''$ with the asymptotic form (5.4) at successive values of $\bar{\eta}$. The expected constant values of $\bar{k}_1, \bar{k}_2, \bar{k}_3$ emerge as $\bar{\eta} \to \infty$, as indicated by dashed lines.

and the positive solution which satisfies (5.3) and approaches $\bar{k}_1 \bar{\eta}^{\frac{5}{4}}$ as $\bar{\eta} \to \infty$ has the form

$$\bar{f} \sim \bar{k}_1 \bar{\eta}^{\frac{5}{4}} + \bar{k}_2 \bar{\eta}^{\frac{3}{4}} + K_0 \bar{\eta}^{\frac{1}{4}} \ln \bar{\eta} + K \bar{\eta}^{\frac{1}{4}} \quad (\bar{\eta} \to \infty), \tag{5.12}$$

where $\bar{k}_2 = -8\bar{q}/5\bar{k}_1$, $K_0 = -3\bar{k}_2^2/10\bar{k}_1$ and $\bar{k}_1 > 0$. Comparison of (5.10) and (5.12) gives $\bar{k}_3 + \bar{k}_4 = K$ and $\delta(\bar{k}_3 - 3\bar{k}_4) = K_0$ with the result that in particular

$$\bar{k}_3 \sim \tfrac{1}{4} K_0 (b - \tfrac{5}{4})^{-1} \quad (b \to \tfrac{5}{4}), \tag{5.13}$$

and since $K_0 < 0$ this shows that $\bar{k}_3$ becomes large and negative as $b \to \frac{5}{4}+$.

The two results (5.9) and (5.13) show that $k_3(b)$ varies from large negative values to large positive values as b rises from $\frac{5}{4}$ to $\frac{3}{2}$, suggesting the existence of a zero of $k_3(b)$ for one value of b in the range $\frac{5}{4} < b < \frac{3}{2}$. Numerical calculations confirmed this and indicated a zero of k_3 at $b \approx 1.36$. These calculations were carried out by solving (5.2), (5.3) for a range of values of b using a fourth-order Runge–Kutta scheme. For each value of b the value of $\bar{q}$ was adjusted iteratively until the algebraic behaviour (5.4) was obtained for large $\bar{\eta}$. The corresponding values of $\bar{k}_1$ and $\bar{k}_3$ were then estimated from the numerical results using the asymptotic formula (5.4). This was done by equating values of $\bar{f}$, $\bar{\eta}\bar{f}'$ and $\bar{\eta}^2\bar{f}''$ from the Runge–Kutta formulae to the values predicted by (5.4); $\bar{k}_4$ was eliminated from these three equations and then the formula for $\bar{k}_2$ used to leave a pair of equations which determined $\bar{k}_1$ and $\bar{k}_3$. Constant forms should be obtained for sufficiently large $\bar{\eta}$ and this was found to be the case, although the close proximity of the algebraic terms in (5.4) leads to relatively slow convergence of $\bar{k}_3$, evident from the typical set of results shown in figure 3. The results are summarized in table 1, and figure 4 shows $\bar{k}_3$ and $\bar{q}$ as functions of b in the

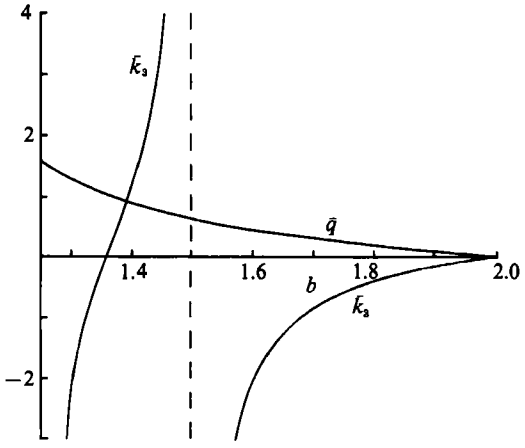

FIGURE 4. Values of $\bar{k}_3$ and $\bar{q}$ in the range $\frac{5}{4} \leqslant b \leqslant 2$ obtained from (5.2)–(5.4).

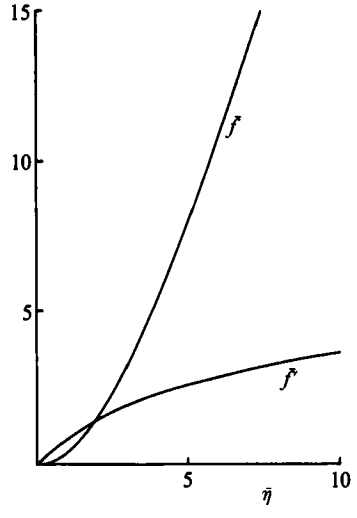

FIGURE 5. Solutions for $\bar{f}$ and $\bar{f}'$ at $b = 1.36$, $\bar{q} = 1.024$.

b	$\bar{q}$	$\bar{k}_1$	$\bar{k}_2$	$\bar{k}_3$
1.300	1.286	1.567	−1.579	−2.3
1.325	1.166	1.478	−1.701	−1.1
1.350	1.062	1.397	−1.877	−0.3
1.360	1.024	1.368	−1.966	0
1.370	0.988	1.339	−2.072	0.3
1.400	0.890	1.258	−2.527	1.1
1.425	0.818	1.197	−3.197	1.9
1.450	0.753	1.141	−4.551	3.5

TABLE 1. Results from the numerical solution of (5.2)–(5.4) in the range $\frac{5}{4} < b < \frac{3}{2}$

extended range $\frac{5}{4} \leqslant b \leqslant 2$, confirming in particular the asymptotic forms predicted by (5.9) and (5.13) as $b \to \frac{3}{2}$ and $b \to \frac{5}{4}$. The solution for $\bar{f}$ at $b = 1.36$ is shown in figure 5 and the corresponding value of $\bar{q}$ is 1.024.

A few remarks on the nature of the solution outside the range $\frac{5}{4} < b < \frac{3}{2}$ should also

be made. Both $\bar{k}_3$ and $\bar{q}$ vanish at $b = 2$, where the relevant solution of (5.2), (5.3) is $\bar{f} = \frac{1}{2}\bar{\eta}^2$, and in $2 < b < 3$ become positive and negative respectively, with $\bar{q} \to -\infty$ as $b \to 3-$. As b decreases below $\frac{5}{4}$, $|\bar{k}_3|$ becomes infinite when the term $\bar{k}_3\bar{\eta}^{b-1}$ coincides with a term $\bar{k}_5\bar{\eta}^{6-5b}$ in the asymptotic form of $\bar{f}$, i.e. when $b = \frac{7}{6}$. From a local analysis it is readily established that $\bar{k}_3 \sim \hat{k}_0(b-\frac{7}{6})^{-1}$ as $b \to \frac{7}{6}$ where $\hat{k}_0 < 0$, indicating another zero of k_3 in the interval $\frac{7}{6} < b < \frac{5}{4}$. Numerical results become progressively more difficult to obtain as b decreases below $\frac{5}{4}$ because an increasing number of terms must be taken into account in the asymptotic form of $\bar{f}$ as $\bar{\eta} \to \infty$. However, it is anticipated that there is an infinite set of zeros of k_3, with one zero in each of the intervals bounded by the points $b = 1 + \frac{1}{2}n^{-1}$ $(n = 1, 2, \ldots)$ at which $|\bar{k}_3|$ becomes infinitely large. Zeros of k_3 for which $b < \frac{5}{4}$ are not relevant to the structure of the singularity for the following reason. In the outer solution (3.1) a term $X^{2a}\psi_2(z)$ in the expansion of the stream function satisfies an equation identical to that for ψ_1 but with an additional inhomogeneous term containing nonlinear products of ψ_1, T_1 and their derivatives. One of the complementary solutions for ψ_2 is ψ_1 with the result that the inhomogeneity generates contributions to ψ_2 proportional to z^{4-3b} and z^{b-1} as $z \to 0$. The former matches with the term involving k_4 in the inner solution for f while the latter generates a correction term in the inner solution of order $X^{5(b-1)/(b+1)}$. This is smaller than the leading term of order $X^{b/(b+1)}$ only if $4b-5 > 0$ and so for the proposed structure to remain consistent it is necessary that $b > \frac{5}{4}$. The most singular form of the solution therefore corresponds to the zero of k_3 in the interval $\frac{5}{4} < b < \frac{3}{2}$. For $b > \frac{3}{2}$ the character of the outer problem for ψ_1 changes because then the first of the two inner asymptotes z^{2-b} and z^{b-1} dominates and there are no solutions for which $\Psi \to 0$ as $z \to 0$. The next zero of k_3 is at $b = 2$ but it corresponds to $q = 0$, $\psi_1 = 0$ and a stream-function profile ψ_0 proportional to z^2 as $z \to 0$, equivalent to a boundary layer which proceeds through x_0 in a regular fashion. The present work does not rule out the possibility of singular structures with $b > \frac{3}{2}$ for boundary-layer developments associated with significantly different initial conditions or boundary conditions, although a structure precisely of Goldstein form ($b = 3$) would only be possible at infinite Froude number when the buoyancy term on the right-hand side of (4.1) is negligible.

The system (5.2), (5.3) has been studied for $b = \frac{5}{3}$ in the context of boundary-layer separation at a free streamline by Ackerberg (1970), and for $b = \frac{3}{2}$ in connection with hypersonic free interactions by Brown, Stewartson & Williams (1975); the solution identified here for thermal boundary-layer flow may also provide a possible alternative structure for the singularity associated with an expansive free interaction in hypersonic flow.

6. Inner temperature field

The inner temperature field and the value of c can now be found by solving (3.10), (3.11) with $b = 1.36$ and f the corresponding solution found above. Here it is convenient to set

$$g(\eta) = \beta(\bar{\alpha}/\alpha)^{c/(b+1)}\bar{g}(\bar{\eta}), \tag{6.1}$$

where $\bar{\eta}$ is defined by (5.1). Then $\bar{g}$ satisfies

$$\bar{g}'' - \frac{\sigma}{b+1}(b\bar{f}\bar{g}' - c\bar{f}'\bar{g}) = 0, \tag{6.2}$$

$$\bar{g}' = 0 \quad (\bar{\eta} = 0), \qquad \bar{g} \sim \bar{\eta}^c \quad (\bar{\eta} \to \infty). \tag{6.3}$$

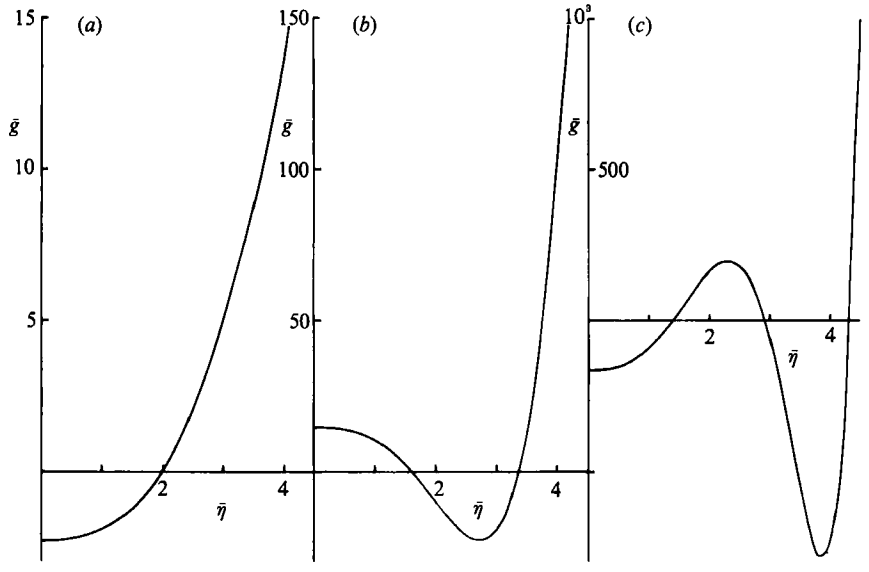

FIGURE 6. The first three eigenfunctions $\bar{g}$ of (6.2), (6.3) for $\sigma = 1$, corresponding to (*a*) $c = 2.20$, (*b*) $c = 4.42$, (*c*) $c = 6.65$.

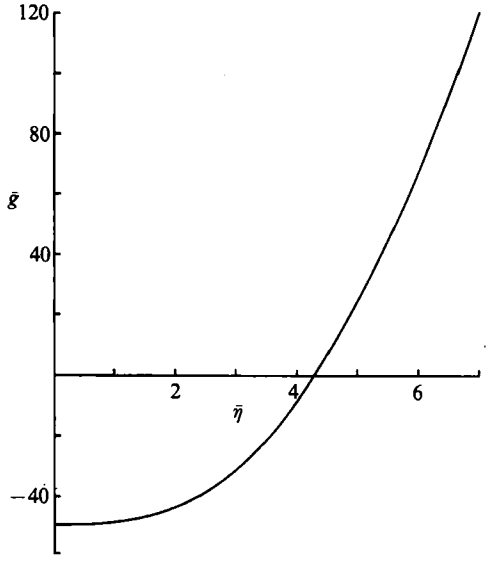

FIGURE 7. The leading eigenfunction $\bar{g}$ of (6.2), (6.3) for $\sigma = 0.1$, corresponding to $c = 2.49$.

Since (6.2) possesses exponentially large solutions as $\bar{\eta} \to \infty$, this constitutes an eigenvalue problem for c and numerical solutions were obtained by computing inwards to the origin using a fourth-order Runge–Kutta scheme, starting from the behaviour $\bar{\eta}^c$ at large $\bar{\eta}$. The value of c was then adjusted iteratively until the wall condition $\bar{g}' = 0$ was satisfied. Results of this procedure including the critical values of c are given for a range of Prandtl numbers in figures 6 and 7, and table 2. Several roots for c were found in some cases although the expectation is that the lowest one is generated at the singularity and is therefore the value which appears in (3.3) and

σ	c
1.5	2.18
1.0	2.20
0.5	2.22
0.1	2.49
0.05	3.07
0.025	4.27
0.01	7.83

TABLE 2. Leading eigenvalues c of the system (6.2), (6.3) with $b = 1.36$

(3.5). It should be noted that the solution of (6.2), (6.3) for which $\bar{g}$ is constant and $c = 0$ can be discounted as it corresponds to the term $T_0(0)$ already incorporated in the inner behaviour (3.3).

An infinite family of roots for c can be expected at a given Prandtl number, as can be seen from a simplified version of (6.2) in which $\bar{f}$ is approximated by the linear form

$$\bar{f} = \bar{\alpha}\bar{\eta}, \tag{6.4}$$

with $b = 1$. Then $\bar{g}$ satisfies

$$\bar{g}'' - \tfrac{1}{2}\sigma\bar{\alpha}(\bar{\eta}\bar{g}' - c\bar{g}) = 0 \tag{6.5}$$

and the solution which avoids exponential growth as $\bar{\eta} \to \infty$ is

$$\bar{g} = \bar{k}\exp(\tfrac{1}{8}\bar{\alpha}\sigma\bar{\eta}^2)\, U\left(-(c+\tfrac{1}{2}), \left(\frac{\bar{\alpha}\sigma}{2}\right)^{\frac{1}{2}}\bar{\eta}\right), \tag{6.6}$$

where U is the parabolic cylinder function defined by Abramowitz & Stegun (1965, p. 686). The outer behaviour $\bar{g} \sim \bar{\eta}^c$ as $\bar{\eta} \to \infty$ is satisfied by choosing $\bar{k} = (\bar{\alpha}\sigma/2)^{-c/2}$ and the wall condition $\bar{g}'(0) = 0$ leads to an infinite set of eigenvalues

$$c = 2n \quad (n = 0, 1, 2, \ldots). \tag{6.7}$$

Again the solution for which $c = 0$ and $\bar{g}$ is constant can be discounted and the relevant solution here is quadratic in $\bar{\eta}$ as $\bar{\eta} \to \infty$.

At this point it is worth noting two minor modifications of the present theory needed to cater for alternative thermal boundary conditions at the wall. First, if the wall temperature is specified rather than the heat transfer, so that

$$T = T_w(x) \quad \text{on} \quad z = 0, \tag{6.8}$$

a similar inner and outer structure is possible in which $T_0(0) = T_w(x_0)$ and the first boundary condition in (6.3) is replaced by

$$\bar{g} = 0 \quad (\bar{\eta} = 0). \tag{6.9}$$

Again an infinite sequence of eigenvalues c is expected and, for the approximation (6.4), result (6.7) is replaced by

$$c = 2n+1 \quad (n = 0, 1, \ldots). \tag{6.10}$$

Generally, however, assuming that $T_w'(x_0) \neq 0$ the form of the inner expansion for T in (3.5) will depend on whether the lowest eigenvalue for c is less than $1+b \approx 2.36$. If it is not, there will be a more significant inner term in (3.5) linear in X corresponding to $c = 1+b$ and generated by the condition $g = -T_w'(x_0)$ at $\eta = 0$, together with the outer requirement $g \sim \beta\eta^{1+b}$ as $\eta \to \infty$.

A second possibility is that the wall heat transfer is specified and non-zero so that

$$\frac{\partial T}{\partial z} = H_w(x) \quad \text{on} \quad z = 0. \tag{6.11}$$

Again a similar inner and outer structure appears to be possible with the leading eigenvalue for c as specified in table 2. However, the inner expansion for T in (3.5) will now contain a more dominant term corresponding to $c = 1$ and a solution of (3.10) for g generated by the condition $g' = H_w(x_0)$ at $\eta = 0$, together with the outer requirement $g \sim \beta\eta$ as $\eta \to \infty$.

Neither of the conditions (6.8) and (6.11) has been tested in a full numerical solution of the horizontal boundary-layer equations to confirm the existence of a singularity in such cases. If such behaviour is possible it must presumably be largely dependent on the manner in which the functions $T_w(x)$ or $H_w(x)$ influence the local Froude number in the boundary layer.

7. Summary and discussion

The nature of a singularity of the horizontal buoyancy-layer equations has been established in which the flow adopts a two-tier structure as $x \to x_0-$. In the outer region which spans the main part of the boundary layer the streamwise pressure and temperature gradients become infinitely large and are given by

$$\frac{\partial p}{\partial x} \sim a(x_0-x)^{a-1}\sigma^{-1}\int_z^\infty T_1\,\mathrm{d}z, \tag{7.1}$$

$$\frac{\partial T}{\partial x} \sim -a(x_0-x)^{a-1}T_1(z), \tag{7.2}$$

as $x \to x_0$, where $a = 2(b-1)/(b+1) \approx 0.305$ and, since $\psi_1(z) < 0$, $T_1 = T_0'\psi_1/u_0$ is negative. Thus the pressure gradient is large and favourable across the layer and the temperature is rapidly increasing. The vertical flow component,

$$w = -\frac{\partial\psi}{\partial x} \sim a(x_0-x)^{a-1}\psi_1(z), \tag{7.3}$$

is negative and the displacement thickness

$$(Uz-\psi)_{z\to\infty} \sim (Uz-\psi_0)_{z\to\infty} - (x_0-x)^a\psi_1(\infty), \tag{7.4}$$

where $\psi_1(\infty) < 0$, is rapidly decreasing as fluid is drawn inwards at the edge of the boundary layer. This fluid is needed to feed the increased streamwise flow near the wall where, since $(b-2)/(b+1) \approx -0.271$ and $f''(0) > 0$ the skin friction is rapidly increasing,

$$\frac{\partial u}{\partial z}(x,0) \sim (x_0-x)^{(b-2)/(b+1)}f''(0), \tag{7.5}$$

and the motion is driven partly by the outer boundary-layer flow and partly by the favourable pressure gradient associated with the behaviour

$$p(x,0) \sim p_0(0) + (x_0-x)^a q, \tag{7.6}$$

where $p_0(0) > 0$ and $q > 0$. The inner temperature field is relatively smooth since $T_1(0) = 0$ and at the wall

$$T(x,0) \sim T_0(0) + (x_0-x)^{c/(b+1)}g(0), \tag{7.7}$$

where $T_0(0) < 0$ and $g(0) < 0$. The value of $c/(1+b)$ is Prandtl-number dependent but for $\sigma \gtrsim 0.3$, c is approximately 2.2 and so $c/(1+b) \approx 0.93$ indicating that relatively little evidence of the singularity will be observed in the wall temperature. The overall structure is quite different from that of the Goldstein singularity in a classical pressure-driven boundary layer and is characterized by the extra freedom here that allows the pressure to evolve interactively within the boundary layer.

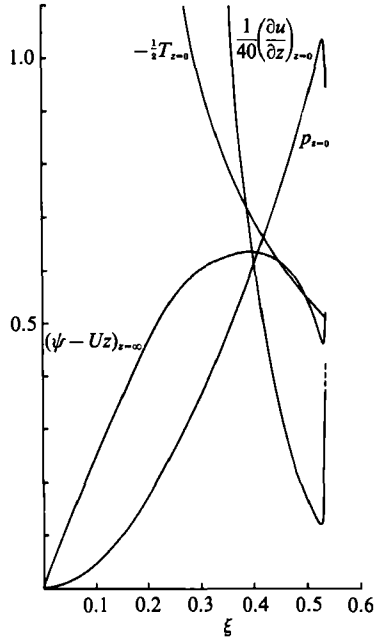

FIGURE 8. Wall pressure, wall temperature, skin friction and displacement for $\mathscr{F} = 1$ and $\sigma = 0.72$ from Gargaro's (1991) numerical solution of the horizontal boundary-layer system (2.10)–(2.15), (2.19). The solution is shown as a function of $\xi = x^{\frac{1}{4}}$ and terminates in a singularity at $\xi \approx 0.53355$.

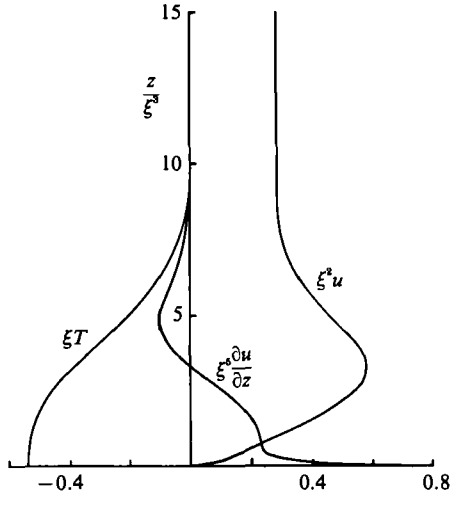

FIGURE 9. Profiles of streamwise velocity, shear and temperature in the boundary layer at $\xi = x^{\frac{1}{4}} = 0.53351$ for $\mathscr{F} = 1$ and $\sigma = 0.72$ from Gargaro's (1991) numerical solution of the system (2.10)–(2.15), (2.19).

All of the preceding qualitative properties of the solution are consistent with the behaviour observed in Gargaro's (1991) numerical solution of the boundary-layer equations. Some of his results for air ($\sigma = 0.72$) and for $\mathscr{F} = 1$, where the solution terminates at $x_0 \approx (0.53355)^4$, are summarized in figure 8. Computations were carried out at extremely small steps in the streamwise direction close to x_0 although no special account was taken of the structure outlined here and indeed the computations can be expected to become progressively less accurate as the singularity is

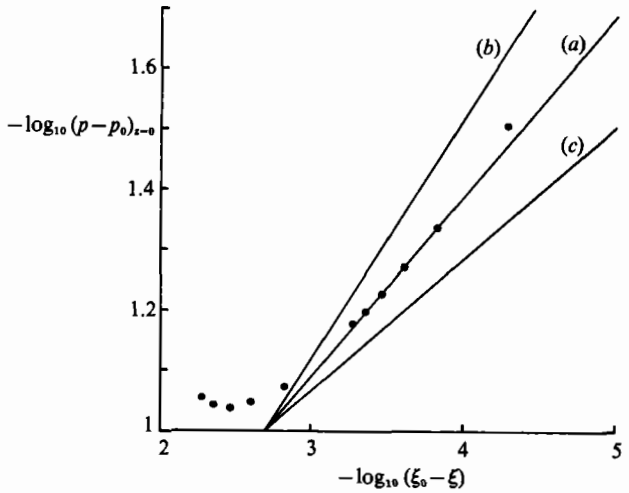

FIGURE 10. Logarithmic plot of the wall pressure for $\mathscr{P} = 1$ and $\sigma = 0.72$ predicted by Gargaro's (1991) numerical computations (•) near the singularity at ξ_0 on the basis that $\xi_0 = 0.533\,55$ and $p_0(0) = 0.945$. Straight lines indicate slopes corresponding to (*a*) the predicted value $a = 0.305$ and (*b*), (*c*) the values $a = \frac{2}{5}$ and $a = \frac{2}{9}$ associated with the upper and lower bounds $b = \frac{3}{2}$ and $b = \frac{5}{4}$ respectively.

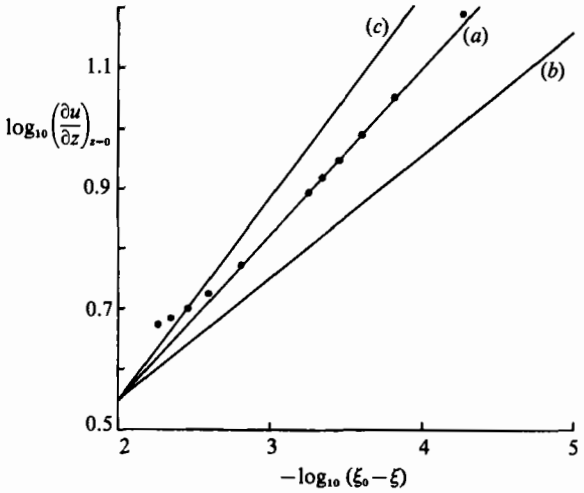

FIGURE 11. Logarithmic plot of the skin friction for $\mathscr{P} = 1$ and $\sigma = 0.72$ predicted by Gargaro's (1991) numerical computations (•) near the singularity at ξ_0 on the basis that $\xi_0 = 0.533\,55$. Straight lines indicate slopes corresponding to (*a*) the predicted value $(2-b)/(1+b) = 0.271$ and (*b*), (*c*) the values $(2-b)/(1+b) = \frac{1}{5}$ and $\frac{1}{3}$ associated with the upper and lower bounds $b = \frac{3}{2}$ and $b = \frac{5}{4}$ respectively.

approached. In particular the inner region is unlikely to be adequately resolved in the z-direction close to the singularity. Figure 9 shows profiles of u, $\partial u/\partial z$ and T in the boundary layer at position $x = (0.533\,51)^4$, just ahead of the singularity. The main quantitative comparisons between the numerical results and those obtained here have been made with a view to confirming the streamwise variation associated with the predicted value of the constant $b \approx 1.36$. Figure 10 shows a comparison of the wall pressure and figure 11 the skin friction. The behaviour predicted by (7.6) and (7.5) with $b = 1.36$ is shown as well as lines corresponding to the two bounding values

$b = \frac{5}{4}$ and $b = \frac{3}{2}$ associated with the theoretical treatment of §5. Overall the agreement appears to be reasonable.

The key to the existence of the singularity is the value of the local Froude number in the boundary layer, as measured by the profiles of velocity and temperature gradient u_0 and T_0' which appear in the outer eigenvalue problem (4.4), (4.5). The Froude number is a measure of the forward momentum provided by the external velocity U relative to the adverse pressure gradient due to buoyancy. Under general circumstances a Froude number for a buoyant thermal flow is based on the ratio

$$u^*/(\alpha^* g^* \{T_0^* - T^*\} z^*)^{\frac{1}{2}} \tag{7.8}$$

(Turner 1973, p. 12) which in the present instance reduces to

$$(\sigma/z|T|)^{\frac{1}{2}} u. \tag{7.9}$$

As the boundary-layer profiles u and T develop, the local Froude number varies until the condition for the existence of the leading eigensolution of (4.4), (4.5) is met and at this point the singularity occurs. In the computations performed by Gargaro the initial jet profile (2.19) corresponds to a Froude number of order $x^{-\frac{3}{4}}$ as $x \to 0$, while the large-x asymptote (2.20) corresponds to a suitably defined finite Froude number proportional to $\mathscr{F}^{\frac{8}{5}}$. Thus for sufficiently low values of $\mathscr{F} = U/Q^{\frac{1}{5}}$ the local Froude number in the boundary layer decreases to the point where the singularity is provoked. In fact, Gargaro found that generally the singularity occurs for a wider range of values of $U/Q^{\frac{1}{5}}$ than the range $\mathscr{F} < \mathscr{F}_0(\sigma)$ corresponding to non-existence of the large-x asymptote (2.20).

The horizontal boundary-layer problem studied by Gargaro is of interest in the context of thermally driven cavity flows. In particular, it is believed to describe the flow in a shallow cavity whose endwalls are maintained at different constant temperatures (Daniels *et al.* 1987). At the cold wall the flow descends as a jet and then its evolution along the bottom insulated wall is initially as a non-buoyant jet which then diffuses and develops on a longer scale into the horizontal boundary layer governed by (2.10)–(2.15) as both buoyancy and an external recirculating flow become significant. An unknown factor in this theory is the strength of the external flow and therefore whether it is sufficiently small to provoke the transition from supercritical to subcritical Froude number. However, there is some evidence that in cavities of moderate aspect ratio the flows emerging from the lower cold and upper hot corners do undergo internal 'hydraulic jumps' of the type described by Turner (1973, p. 64). These have been discussed in the context of transient motions in laterally heated square cavities by Ivey (1984) and observed in numerical simulations at high Rayleigh numbers by, for example, Winters (1983), Chenoweth & Paolucci (1986) and Gaskell & Wright (1987).

Whether the terminal boundary-layer behaviour described in the present work is physically realistic and, indeed, is the precursor of an internal hydraulic jump from supercritical to subcritical flow remains to be seen. One possibility is that the singular form of the boundary layer described here adjusts on a shorter streamwise lengthscale, possibly encompassing separation from the wall, to enable the flow to proceed downstream. Although the skin friction increases as the singularity is approached this initial trend might be reversed as streamwise gradients become more severe. On the other hand, and perhaps more likely, the singularity of the boundary-layer equations may herald a complete breakdown of the theory just as the Goldstein singularity does in the case of a classical boundary-layer flow when interaction with the mainstream is excluded. A mechanism for free interaction would then appear to

be necessary upstream and indeed for sufficiently large Froude numbers such mechanisms exist in the form of the triple-deck or, for jet-flow, the double-deck structure of Smith & Duck (1977).

REFERENCES

ABRAMOWITZ, M. & STEGUN, I. A. 1965 *Handbook of Mathematical Functions*. Dover.

ACKERBERG, R. C. 1970 *J. Fluid Mech.* **44**, 211.

ACKROYD, J. A. D. 1976 *Proc. R. Soc. Lond.* A **352**, 249.

AIHARA, T., YAMADA, Y. & ENDO, E. 1972 *Intl J. Heat Mass Transfer* **15**, 2535.

AL-ARABI, M. & EL-RIEDY, M. K. 1976 *Intl J. Heat Mass Transfer* **19**, 1399.

BANDROWSKI, J. & RYBSKI, W. 1976 *Intl J. Heat Mass Transfer* **19**, 827.

BEJAN, A., AL-HOMOUD, A. A. & IMBERGER, J. 1981 *J. Fluid Mech.* **109**, 283.

BROWN, S. N., STEWARTSON, K. & WILLIAMS, P. G. 1975 *Proc. R. Soc. Edin.* **74A**, 271.

CHENOWETH, D. R. & PAOLUCCI, S. 1986 *J. Fluid Mech.* **169**, 173.

CLIFTON, J. V. & CHAPMAN, A. J. 1969 *Intl J. Heat Mass Transfer* **12**, 1573.

DANIELS, P. G., BLYTHE, P. A. & SIMPKINS, P. G. 1987 High Rayleigh number thermal convection in a shallow laterally heated cavity. *AT & T Bell Lab. Tech. Mem.* (unpublished).

FAW, R. E. & DULLFORCE, T. A. 1981 *Intl J. Heat Mass Transfer* **24**, 859.

GARGARO, R. J. 1991 Thermally-driven shallow cavity flows. PhD thesis, City University, London.

GASKELL, P. H. & WRIGHT, N. G. 1987 In *Proc. 5th Intl Conf. Numerical Methods for Thermal Problems, Montreal* (ed. R. W. Lewis & K. Morgan). Swansea: Pineridge.

GILL, W. N., ZEH, D. W. & CASAL, E. DEL 1965 *Z. Angew Math. Phys.* **16**, 539.

GLAUERT, M. B. 1956 *J. Fluid Mech.* **1**, 625.

GOLDSTEIN, R. J. & LAU, K.-S. 1983 *J. Fluid Mech.* **129**, 55.

GOLDSTEIN, R. J., SPARROW, E. M. & JONES, D. C. 1973 *Intl J. Heat Mass Transfer* **16**, 1025.

GOLDSTEIN, S. 1948 *Q. J. Mech. Appl. Maths.* **1**, 43.

HARTREE, D. R. 1937 *Math. Proc. Camb. Phil. Soc.* **33**, 223.

HATFIELD, D. W. & EDWARDS, D. K. 1981 *Intl J. Heat Mass Transfer* **24**, 1019.

HUNT, R. & WILKS, G. 1980 *J. Fluid Mech.* **101**, 377.

INGHAM, D. B. 1985 *Proc. R. Soc. Lond.* A **402**, 109.

IVEY, G. N. 1984 *J. Fluid Mech.* **144**, 389.

JONES, D. R. 1973 *Q. J. Mech. Appl. Maths* **26**, 77.

KERR, C. N. 1980 *Intl J. Heat Mass Transfer* **23**, 247.

MERKIN, J. H. 1969 *J. Fluid Mech.* **35**, 439.

MERKIN, J. H. 1983 *Q. J. Mech. Appl. Maths* **36**, 71.

MESSITER, A. F. 1970 *SIAM J. Appl. Maths* **18**, 241.

MESSITER, A. F. & LINAN, A. 1976 *Z. Angew Math. Phys.* **27**, 633.

PATTERSON, J. C. & ARMFIELD, S. W. 1990 *J. Fluid Mech.* **219**, 469.

PERA, L. & GEBHART, B. 1973 *Intl J. Heat Mass Transfer* **16**, 1131.

RESTREPO, F. & GLICKSMAN, L. R. 1974 *Intl J. Heat Mass Transfer* **17**, 135.

ROSS, S. L. 1964 *Differential Equations*. Blaisdell.

ROTEM, Z. & CLAASSEN, L. 1969 *J. Fluid Mech.* **39**, 173.

SIMPKINS, P. G. & CHEN, K. S. 1986 *J. Fluid Mech.* **166**, 21.

SMITH, F. T. 1982 *IMA J. Appl. Maths* **28**, 207.

SMITH, F. T. & DUCK, P. W. 1977 *Q. J. Mech. Appl. Maths* **30**, 143.

STEWARTSON, K. 1954 *Math. Proc. Camb. Phil. Soc.* **50**, 454.

STEWARTSON, K. 1958 *Z. Angew Math. Phys.* **9**, 276.

STEWARTSON, K. 1970 *J. Fluid Mech.* **44**, 347.

STEWARTSON, K. & WILLIAMS, P. G. 1969 *Proc. R. Soc. Lond.* A **312**, 181.

TURNER, J. S. 1973 *Buoyancy Effects in Fluids*. Cambridge University Press.

WILKS, G. 1974 *J. Fluid Mech.* **62**, 359.

WINTERS, K. 1983 In *Numerical Methods in Heat Transfer* (ed. R. W. Lewis, K. Morgan & B. A. Schrefler), ch. 7. Wiley.